

Solute distribution at the solid-liquid interface during steady-state peritectic solidification

D. H. ST. JOHN, L. M. HOGAN

Department of Mining and Metallurgical Engineering, University of Queensland, St. Lucia 4067, Australia

The solute distributions at the solid-liquid interface during steady-state directional solidification of two contrasting peritectic systems were examined in detail by electron probe microanalysis. In the Al-Al₃Ti system the peritectic transformation plays a negligible part in the solidification reaction whereas in the Cd-Cd₃Ag system the peritectic transformation dominates. Knowing this, the solid-liquid interface profile during solidification can be predicted with reasonable accuracy on the assumption of equilibrium at all points on the solid-liquid interface. In the Cd-Cd₃Ag system the composition of the peritectic product is rapidly equilibrated by solid-state diffusion. A diffusion coefficient is estimated.

1. Introduction

When a two-phase peritectic alloy, of composition such as C_x in Fig. 1, is unidirectionally solidified under steady-state conditions, the solid-liquid interface shape will normally assume the type of profile shown in Figs. 2 and 3. Primary β phase dendrites grow roughly parallel to the applied temperature gradient with their tips far in advance of an α phase interface. The lead distance will depend on alloy composition (within the peritectic range) and applied temperature gradient, G . Boettinger [1] has shown that the lead distance of the primary dendrites can be reduced by applying a sufficiently high ratio of G to growth velocity (V), but that complete suppression of the primary dendrites does not lead to steady-state growth.

Uhlman and Chadwick [2] analysed the probable solute distribution in the melt during steady-state growth at low G/V ratios and found that the growth patterns observed in a silver-tin alloy were in general agreement with their predictions. An opportunity to test their hypothesis quantitatively was taken during experiments to compare the freezing behaviour of alloys in two peritectic systems, Al-Al₃Ti and Cd-Cd₃Ag [3]. Alloys from each system were grown unidirectionally at slow

rates, quenched during growth, and scanned by electron probe microanalysis over longitudinal sections through the solid-liquid interface. Probe traces along isotherms parallel to the solid-liquid interface were also taken, in the patterns shown in Figs. 2 and 3.

Uhlmann and Chadwick proposed that the α interface should be concave towards the melt in order to satisfy equilibrium conditions, but observation of the interface shape can become confused by strong lateral branching of the primary dendrites. In the Al-Al₃Ti system this problem is minimized because the primary Al₃Ti is strongly anisotropic and the dendrites grow as flat plates [4], as in Fig. 4. It is therefore convenient to use this system to consider the "ideal" solute distribution during steady-state peritectic solidification, before comparing this with experimental observations.

2. Predicted solute distribution in an Al-Al₃Ti alloy

Consider an alloy of composition C_x (Fig. 1) unidirectionally solidified under a linear applied temperature gradient $G^{\circ}\text{C cm}^{-1}$. In the simplest case, ignoring dendrite branching, the solid-liquid inter-

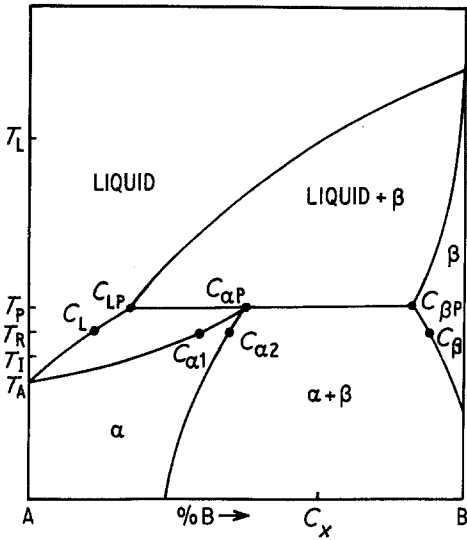


Figure 1 Hypothetical peritectic phase diagram, showing symbols used for phases, compositions and temperatures. Alloys of initial compositions between C_{LP} and $C_{\alpha P}$ are hypo-peritectic alloys; between $C_{\alpha P}$ and $C_{\beta P}$ are hyper-peritectic alloys; between C_{LP} and $C_{\beta P}$ are peritectic alloys; and less than C_{LP} are non-peritectic alloys. C_{LP} is the peritectic limit, and $C_{\alpha P}$ is the peritectic point.

face formed will be of the shape shown in Fig. 5a, which is in broad agreement with the concave interface predicted by Uhlmann and Chadwick. It has been shown [3] that under steady-state growth conditions all points on the solid-liquid interface are at equilibrium as given by the phase diagram, within the accuracy of measurement. That is, the pro-peritectic β phase forms dendrites lying roughly parallel to the overall growth direction, with their tips lying on the isotherm at the alloy liquidus temperature, T_L . For each isotherm between T_L and T_P the liquid in contact with a β dendrite will have a composition given by the liquidus at that

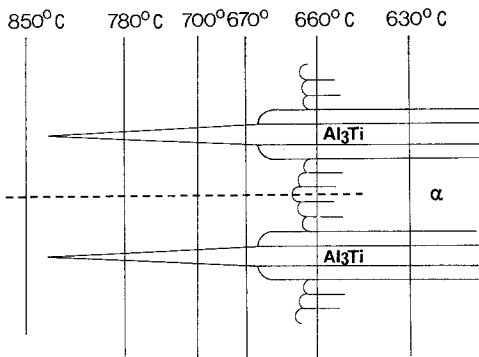


Figure 2 Schematic solid-liquid interface in an Al- Al_3Ti alloy solidified unidirectionally, showing the positions of all probe traces.

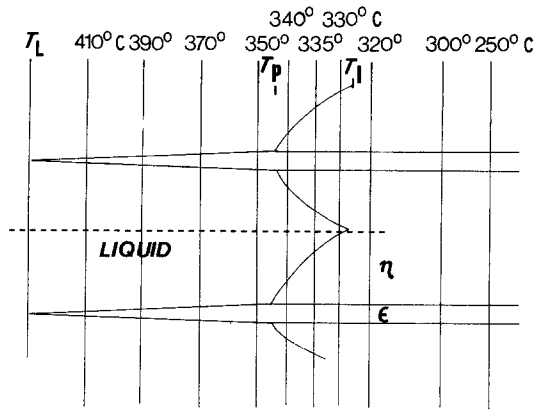


Figure 3 Schematic solid-liquid interface in the cadmium-silver alloy showing positions of all probe traces.

temperature. This composition is maintained by the slow lateral growth of the β dendrites, which withdraws solute B from the adjacent melt, and as a first approximation it can be assumed that diffusion maintains a constant melt composition along each isotherm. Then the liquid between adjacent dendrites will change composition from C_x at the dendrite tips to C_{LP} at T_P , following the β liquidus.

At T_P solid α will form by the peritectic reaction

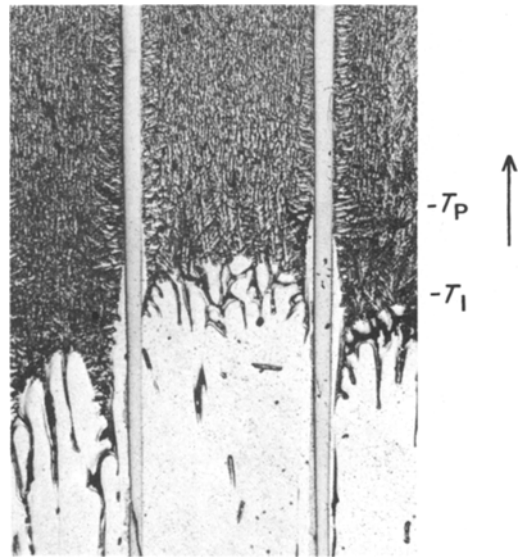
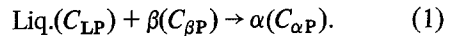


Figure 4 Quenched interface of an Al-0.6% Ti alloy solidified unidirectionally at $5 \mu\text{m sec}^{-1}$. A peritectic envelope is detectable between T_P and T_I and a quasi-planar (cellular) interface forms at T_I . The arrow shows growth direction. $\times 82.5$.

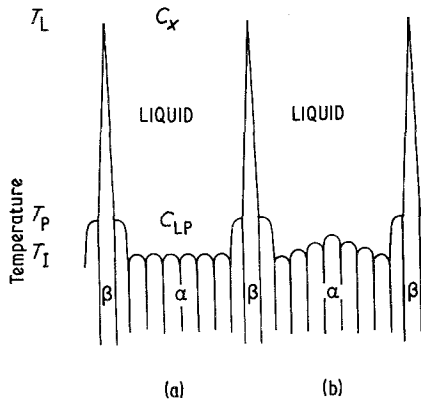


Figure 5 Schematic solid-liquid interface profile of Al-Al₃Ti. (a) Isothermal liquid- α interface as assumed. (b) Actual convex liquid- α interface due to transverse concentration gradients in the liquid.

Nucleation is unnecessary since α phase is already present in steady-state growth and an envelope of α encloses the β at lower temperatures. This three-phase reaction establishes the melt composition as C_{LP} across the isotherm at T_P .

Alpha phase can also form by crystallization from melt of any composition between C_{LP} and pure A, without any reaction with the β phase, and it can be expected that a quasi-planar α -liquid interface will form at some temperature T_I below T_P (Fig. 5a). If convection is absent and the growth rate ($V \mu\text{m sec}^{-1}$) is slow this interface will be equivalent to a planar interface formed during steady-state growth from a melt of uniform composition C_{LP} , with effective distribution coefficient $k_e = 1$, so that the solid α will be of the same composition as the melt from which it forms. This requires that the melt in contact with the α interface is of composition C_{LP}/k , where k is the equilibrium distribution coefficient. Between T_P and T_I a composition gradient from C_{LP} to C_{LP}/k is established in the melt by absorption of B atoms into the growing solid α . The interface temperature T_I is then obtained from

$$\frac{C_{LP} - C_{LP}/k}{T_P - T_I} = m \quad (2)$$

where m is the slope of the α liquidus. More simply, T_I can be read from the phase diagram as the liquidus temperature of melt of composition C_{LP}/k . The relevant portion of the Al-Al₃Ti phase diagram is shown in Fig. 6.

For Al-Al₃Ti, $T_P = 665^\circ\text{C}$, $C_{LP} = 0.15\%$

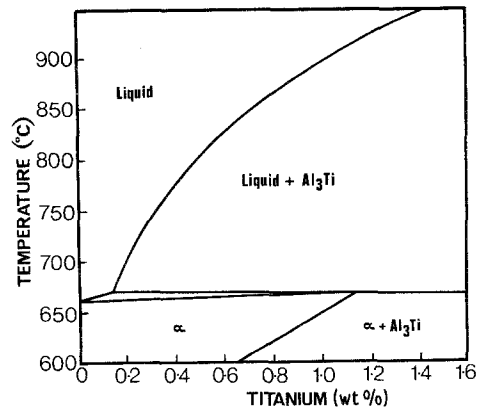


Figure 6 Al-Al₃Ti phase diagram. Al₃Ti forms with 37.5 wt % titanium.

titanium, $k = C_{\alpha P}/C_{LP} = 7.7$, hence $C_{LP}/k = 0.15/7.7 = 0.019\%$ titanium. This point on the α liquidus occurs at temperature $T_I = 661^\circ\text{C}$.

We expect the peritectic reaction to form an envelope about the properitectic β dendrites at the the 665°C isotherm. The envelope will thicken progressively at lower temperatures by the diffusion-controlled peritectic transformation [3] and solidification will be completed at the 661°C isotherm by the presence of a planar liquid- α interface.

3. Observed solute distribution in an Al-0.6% Ti alloy

An Al-0.6% Ti alloy* was grown unidirectionally at $V = 5 \mu\text{m sec}^{-1}$ in a temperature gradient $G = 200^\circ\text{C cm}^{-1}$. Experimental procedure was as in the Appendix and in [3]. The specimen was quenched during solidification and sectioned longitudinally to expose an interface as in Fig. 4. In general the Al₃Ti primary plates do not grow parallel to the overall growth direction and Fig. 4 shows a selected point on the interface at which two adjacent plates grew parallel to each other and to the direction of heat extraction. The distribution of titanium was observed by a longitudinal probe trace, shown dotted in Fig. 2, midway between the two plates, and by transverse traces at the various isotherms shown. The longitudinal trace is shown in Fig. 7. As predicted, the melt composition changes from the alloy composition, $C_x = 0.6\%$ titanium, near the dendrite tips approximately 15 mm ahead of the α interface, to $C_{LP} = 0.15\%$ titanium at T_P , then drops sharply

*All composites are given in wt %.

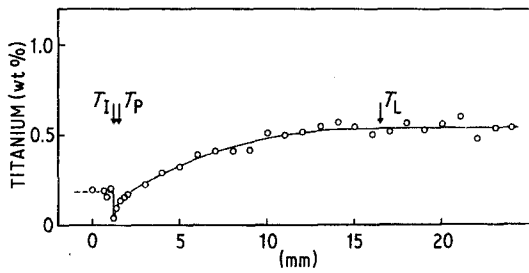


Figure 7 Longitudinal probe trace on Al-0.6% Ti alloy (dotted in Fig. 2). $V = 5 \mu\text{m sec}^{-1}$. Each point represents the average of 30 spot counts, each for 10 seconds, within a given area. Spot size $\approx 1 \mu\text{m}$.

to approximately $C_{LP}/k = 0.02\%$ titanium in the liquid adjacent to the α interface. The lowest measured value was actually 0.05% titanium. The solidified phase has the composition 0.15% titanium = C_{LP} . Between T_L and T_P the measured points corresponded with the Al_3Ti liquidus.

Fig. 8a shows a representative lateral trace at the 780°C isotherm. There is considerable scatter due to coring, but depletion of titanium adjacent to the Al_3Ti dendrite surfaces is evident. The centre-line composition was in agreement with the longitudinal trace in all lateral traces. The titanium

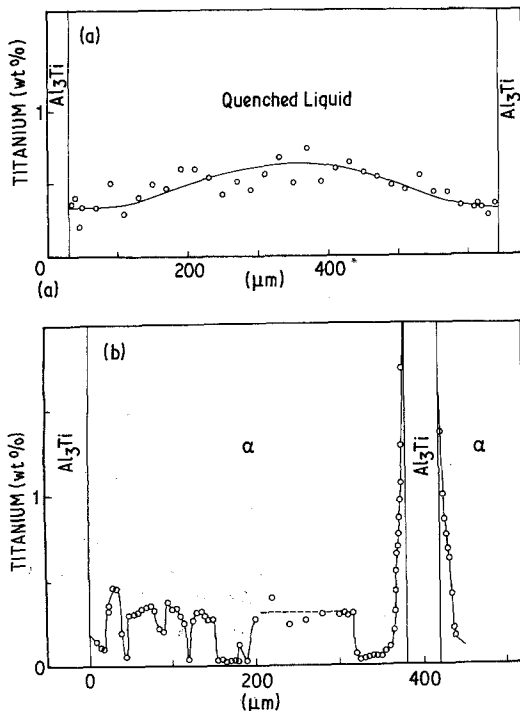


Figure 8 Lateral traces on Al- Al_3Ti . Each point is equivalent to a ($1 \mu\text{m}$) spot count of 10 seconds. (a) 780°C isotherm; (b) 660°C isotherm.

depletion near the Al_3Ti dendrites was more pronounced at the 850°C isotherm, less pronounced at 700°C and undetectable at 670°C . Evidently the rate of thickening of the primary dendrites decreased progressively with distance behind their tips.

Fig. 8b shows a lateral trace at 660°C , just behind the quenched interface. The α interface is cellular (Fig. 4) with composition varying between about 0.4% titanium and near zero at the cell boundaries, compatible with 0.15% titanium measured at the centre-line (Fig. 7). At about $12 \mu\text{m}$ from the Al_3Ti - α interface the titanium content rises rapidly, following the α solidus to 1.15%, which is the composition of the α phase in equilibrium with Al_3Ti at 665°C . The maximum in Fig. 8b is higher than this, due to titanium pick-up from the Al_3Ti in the $1 \mu\text{m}$ beam, but more precise measurements are shown in Fig. 9, which shows the development of the titanium-rich layer between the 665°C and 661°C isotherms. The α in contact with Al_3Ti remained consistently at the equilibrium composition of 1.15% titanium while the layer thickened progressively at a decreasing rate as the temperature fell, reaching a maximum thickness of $12 \mu\text{m}$. (Fig. 9).

It has been shown elsewhere [3] that less than $1 \mu\text{m}$ of this layer thickness is formed by the peritectic transformation, in which α reacts with the liquid by diffusion through the envelope. The remainder is formed by direct precipitation from the liquid, as the temperature falls from T_P and T_I . At T_I the remaining liquid, reduced to 0.02% titanium, transforms to α under the plane interface constitutionally undercooled condition discussed

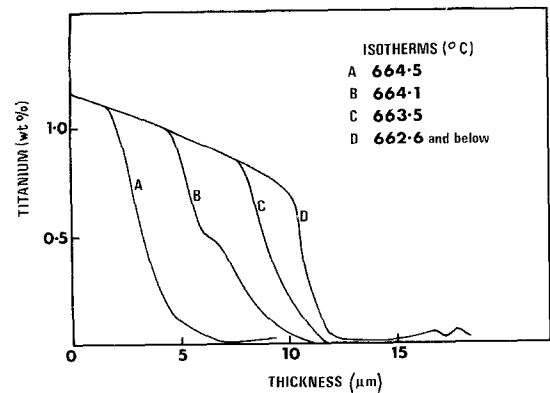


Figure 9 Probe traces of the α peritectic envelope in Fig. 4 at the series of isotherms indicated. Further thickening of the wall is negligible below 662.6°C .

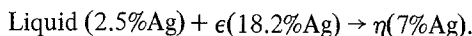
above. However, this last-formed interface is not planar, as sketched in Fig. 5a, but convex, as in Fig. 5b and detectable in Fig. 4. This is because, at any interface between T_P and T_I , the depletion of titanium due to thickening of the side layers results in a concentration gradient in the melt, with maximum percentage titanium at the midpoint between Al_3Ti plates. If the solid α at the interface is to have the same composition as the liquid T_P , then the interface shape must be convex. In terms of this detail, therefore, the interface is convex, rather than concave as predicted earlier [2].

The interface profile described above is characteristic of a peritectic system in which the peritectic transformation plays a negligible part in the formation of the secondary (α) phase. By contrast, in the Cd–Cd₃Ag system the secondary phase is formed almost entirely by the peritectic transformation. The effect of this is to produce a markedly different interface profile.

4. Predicted solute distribution in a Cd–8% Ag alloy

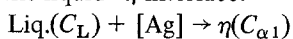
Measurements of solute distribution in the Cd–Cd₃Ag system (Fig. 10) are complicated by the branched dendrite morphology of the pro-peritectic ϵ phase (Fig. 11) and it is useful first to consider the idealized profile shown in Fig. 3. This represents steady-state growth from right to left, maintained by a temperature gradient moving from right to left along the length of the specimen. Probe traces taken on the quenched specimen are superimposed. Assume [3] that solid and liquid are in equilibrium at all points on the interface.

Epsilon dendrites project from the interface with their tips at T_L ($\approx 440^\circ C$ for 8% silver). Behind the tips thickening of the silver-rich dendrites extracts silver from the melt so that the melt composition changes along the ϵ liquidus from 8% silver at T_L to 2.5% silver at T_P ($343^\circ C$). At T_P the peritectic reaction occurs, marking the beginning of the peritectic envelope:



At lower temperatures there is no further contact between ϵ and the liquid and thickening of the η envelope proceeds by the peritectic transformation:

at the liquid– η interface:



at the η – ϵ interface: $\epsilon(C_\beta) \rightarrow \eta(C_{\alpha 2}) + [Ag]$,

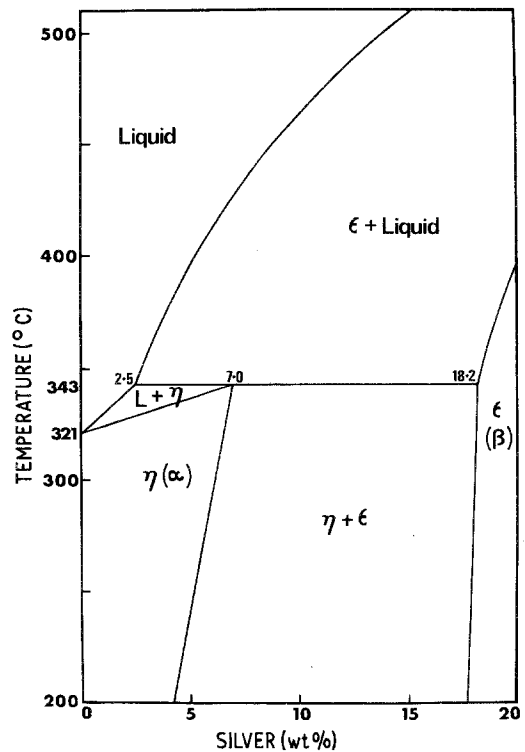


Figure 10 The ϵ – η portion of the cadmium–silver phase diagram. η and ϵ phases correspond to α and β in Fig. 1.

where the composition subscripts refer to Fig. 1, equating η with α and ϵ with β . $[Ag]$ represents a diffusion flow of silver from the ϵ phase to the Liq.– η interface. The transformation continues as temperature falls from T_P to T_I , with the liquid composition (C_L) following the η liquidus while the η phase in contact with the liquid follows the η solidus ($C_{\alpha 1}$). At the η – ϵ interface the η composition should remain close to 7% silver ($C_{\alpha 2}$). Some equalization of the η phase composition should occur by solid state diffusion after completion of solidification.

The rate of thickening of the envelope decreases with increasing diffusion distance [3] so that the Liq.– η interfaces curve back to meet at a point as the last liquid freezes, at temperature T_I . Since direct precipitation of η from the liquid occurs to a negligible extent in this system [3], the “planar” interface observed at T_I in the Al–Al₃Ti system is not to be expected.

If melt composition is assumed constant along each isotherm in Fig. 3 the composition variation along the longitudinal trace can be predicted from the equilibrium diagram (Fig. 10) as in Fig. 12. Between T_L and T_P the melt composition should

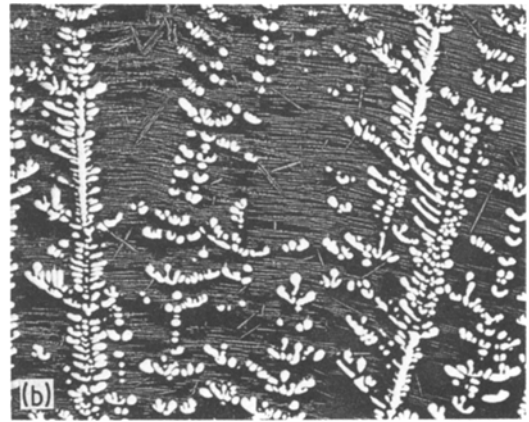
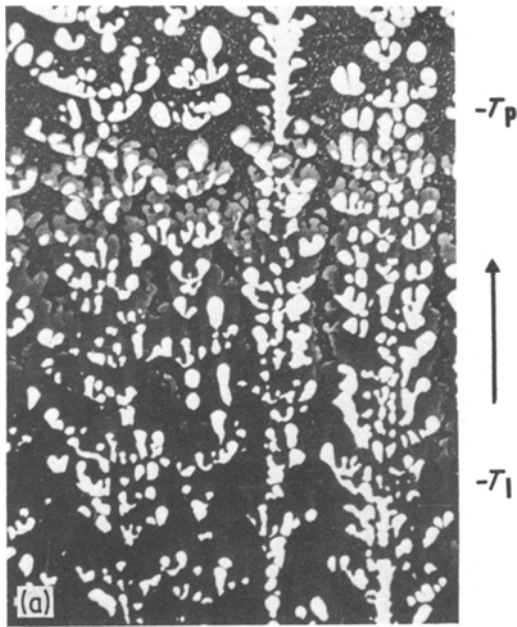


Figure 11 Longitudinal sections of solid-liquid interface in Cd-8% Ag alloy. $V = 5 \mu\text{m sec}^{-1}$, $G = 128^\circ \text{C cm}^{-1}$. (a) Etchant reveals peritectic product as grey-etching "shadows" in a band between 343°C (T_P) and 330°C (T_I). Volume fraction of white-etching ϵ phase decreases below T_I . $\times 43$. (b) Section near the tips of the primary Cd_3Ag dendrites showing fine Cd_3Ag dendrites in the quenched liquid. $\times 56$. The arrow indicates growth direction.

follow the ϵ liquidus from 8% silver to $C_{LP} = 2.5\%$ silver. Between T_P and T_I the silver content should decrease more rapidly down the η liquidus. For steady-state growth the average silver content in the solid η must equal the silver content in the liquid at $T_P = 2.5\%$ Ag. The corresponding liquidus composition is $2.5/k$ where $k = 7/2.5 = 2.8$. Hence the last liquid to freeze should contain approximately $2.5/2.8 = 0.9\%$ silver, and the corresponding temperature, $T_I \approx 329^\circ \text{C}$. The solid η formed from this liquid should then be $kC_L = 2.8 \times 0.9 = 2.5\%$ silver. Below T_I solid-state dif-

fusion should equalize solute concentration in the η phase and the curve should rise towards the $C_{\alpha 2}$ saturation line.

5. Measured solute distribution in Cd-8% Ag alloy

Experimental testing of these predictions was complicated by the microstructure (Fig. 11), in which the properitectic dendrites branch widely and the quenched melt between the dendrites was two-phase. Quenching did not suppress ϵ dendrite formation, so that the quenched melt contained fine ϵ dendrites (Fig. 11b) in decreasing proportion as the melt composition changed from 8% towards

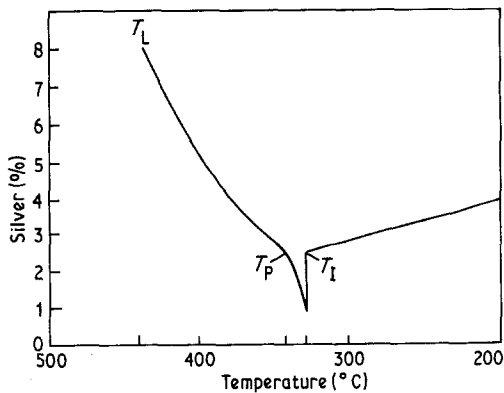


Figure 12 Predicted result of longitudinal probe trace in Cd-8% Ag alloy (dotted trace in Fig. 3). The prediction assumes equilibrium between liquid and solid at all points on the solid-liquid interface.

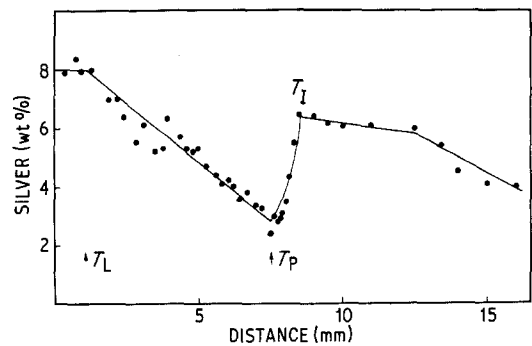


Figure 13 The measured longitudinal probe trace in Cd-8% Ag alloy. Each point represents a 100 second count on an area $40 \mu\text{m}$ square at the position indicated.

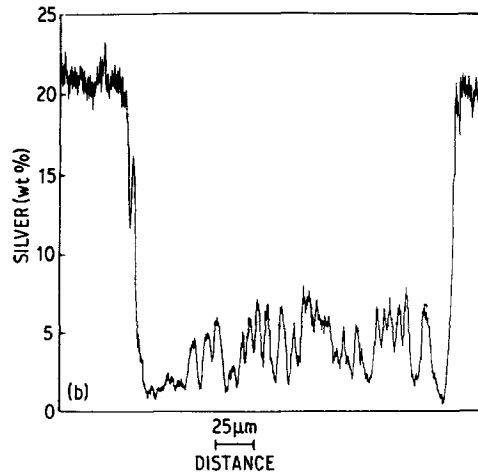
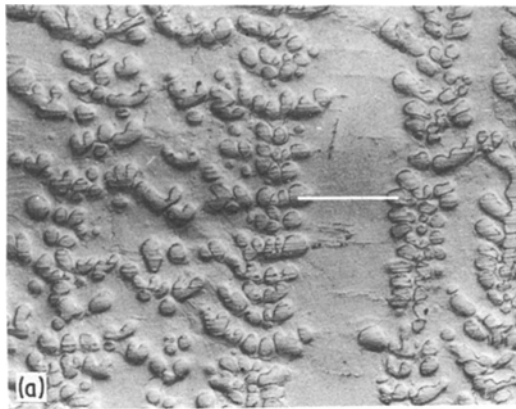


Figure 14 (a) Unetched longitudinal section of Cd-8% Ag alloy showing position of transverse probe trace at the 370° C isotherm. ϵ dendrites are in relief. $\times 90$. (b) Transverse probe trace showing cored η between dendrites.

2.5% silver. In addition, the η phase matrix was heavily cored. Hence, in order to determine the average melt composition at the moment of quenching, probe counts were taken from areas 40 μm square at points midway between primary dendrites (dotted line, Fig. 3). The average spacing between primary dendrite stems was about 100 μm , so that this technique gave a reasonable sampling of the melt between T_L and T_P , but below T_P the test areas overlapped the Liq.- η interface. The results in Fig. 13 show that scatter was reduced to reasonable proportions. Fig. 13 differs substantially from Fig. 12 below T_P and further information was obtained from lateral traces, using a 1 μm probe, at the temperature isotherms shown in Fig. 3. Typical traces are shown in Figs. 14 and 15, just above and just

below T_P . Discussion of these results requires reference to the microstructures.

Fig. 11a shows the Liq.- η interface between T_P (343° C) and T_I ($\approx 330^\circ\text{C}$). The η phase peritectic product T_P appears first as grey-etching "shadows" at the forward tips of the white-etching ϵ dendrite branches. In the fully solid portion at the foot of the photograph η etches black. Apparently the peritectic η nucleates repeatedly at the tips, where the peritectic temperature will first be reached, then spreads back towards the primary stem to enclose the ϵ in a complete peritectic envelope. Channels of quenched liquid can be seen penetrating between successive pairs of primary dendrites and terminating at between 329 and 330° C.

The liquid channels were of variable width not

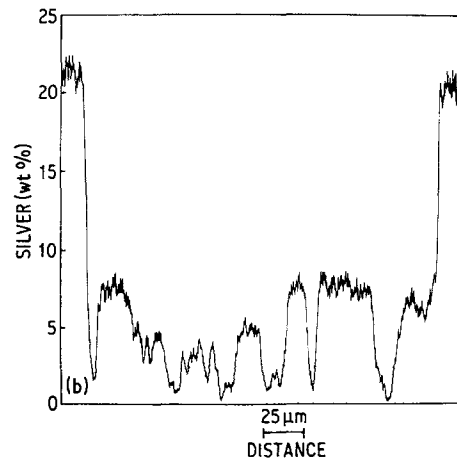
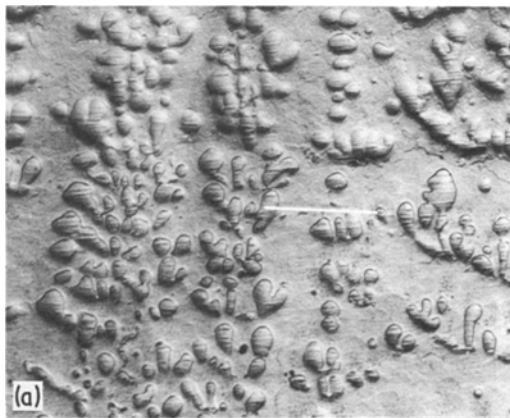


Figure 15 (a) Cd-8% Ag. Position of transverse trace at 340° C. $\times 90$. (b) Transverse trace showing peritectic (7.5% silver) and quenched liquid (smaller peaks) between ϵ peaks.

exceeding $40\ \mu\text{m}$, so that between T_P and T_I the traverse of Fig. 13 incorporated a substantial proportion of η phase from the peritectic envelope and the curve shows the silver content rising rapidly to about 6% silver. This portion of the curve is not relevant, therefore, in predicting the quenched liquid composition, but it peaks at the predicted T_I value of about 329°C and indicates that the η phase at T_I contains 6% silver. The liquid composition would be expected to conform with Fig. 12. Below T_I the curve in the fully solid region tapers off to lower silver contents, which appears to correspond with equilibration along the $C_{\alpha 2}$ line. The slow growth rate ($5\ \mu\text{m}\ \text{sec}^{-1}$) ensures that the solidified material is held for long periods at high temperatures, where solid state diffusion can occur at appreciable rates.

Further information can be obtained from the transverse probe traces. Fig. 14b is a trace at 370°C , 27°C above T_P , in the position shown in the unetched micrograph of Fig. 14a. The ends of the trace intercept primary ϵ dendrites and indicate a cored structure with an average silver content above 20%, a little higher than the equilibrium value at 370°C . At this level the fine ϵ dendrites in the quenched liquid are relatively sparse and none were intercepted. The trace across the η phase matrix shows severe coring, with silver content varying from about 7% maximum to minima below 1% Ag. At 370°C the equilibrium silver content in the melt is 3.6%, which is compatible with the trace. The 7% silver maxima correspond approximately to the peritectic composition and the minima to the η liquidus composition of 0.9% silver at T_I , so that it would appear that the composition fluctuations result from cored cellular growth of the η phase as the temperature fell from T_P to T_I during quenching. The peaks represent the centres of cells which nucleated from the melt as the temperature fell past T_P , where the η solidus composition is 7% silver. As the cells grew falling temperature the deposited η phase followed a non-equilibrium solidus line displaced to the right of the equilibrium η solidus (Fig. 10). Thus the intercellular liquid would be severely depleted in silver before final solidification in the neighbourhood of T_I . The heavier silver depletion adjacent to the ϵ phase is evidence of active growth of the latter.

Fig. 15 is a trace at 340°C , just below T_P . The ends of the trace intercept primary ϵ branches and, in addition, the tip of an ϵ branch has been inter-

cepted towards the right-hand end of the trace. At this tip the peritectic reaction has commenced and a broad peak at 7% silver indicates the formation of the η peritectic product. Two other broad peaks correspond to a peritectic product less readily identifiable in the micrograph. The lower peaks represent quenched liquid and the range from 5% silver to less than 1% silver is compatible with the equilibrium liquid composition of about 2% silver at 340°C . At 335°C a lower maximum was recorded in the quenched liquid, of about 4% silver, so that the transverse traces support the prediction in Fig. 12 that the melt composition should follow the η liquidus between T_P and T_I . This means that the η phase in the peritectic envelope is gaining silver from the melt as well as from the ϵ phase.

Fig. 16 shows the trace at $T_I = 330^\circ\text{C}$, where solidification is just completed. The trace confirms the observation in Fig. 13 that the solid η at this point has an average composition of about 6% silver, compared with 2.5% silver predicted in Fig. 12. However, Fig. 12 refers to the last drop of liquid to freeze, which should contain 0.9% silver at T_I , at which temperature the η solidus composition is 2.5% silver. The two minima in Fig. 16 correspond to two "tails" in the liquid channel (Fig. 11) and suggest that liquid of this composition did indeed survive and froze without appreciable change of composition. But the adjacent solid interface composition of 6% silver lies on the (η - ϵ) boundary ($C_{\alpha 2}$), suggesting that solid-state diffusion is sufficiently fast to maintain equilibrium between η and ϵ phases when the amount of liquid remaining is too small to be influential. The build-up of silver content in the η phase is assisted by withdrawing silver from the remaining liquid, and it is perhaps coincidental that the melt composition appears to follow the liquidus between T_P and T_I . The high rate of solid-state diffusion is also indicated by transverse traces at 330, 300, and 250°C , which show progressive homogenization of the solid η phase with average silver content falling from 6% towards 4% silver, as in Fig. 13.

Fig. 12 predicted a rising silver content over this range, on the assumption that the solid η phase at the solid-liquid interface should lie on the η solidus ($C_{\alpha 1}$) at T_I (2.5% silver). Figs. 13 and 16 show that instead the η phase at this point lies on the $C_{\alpha 2}$ saturation limit and that, during subsequent cooling, the η phase follows down the $C_{\alpha 2}$

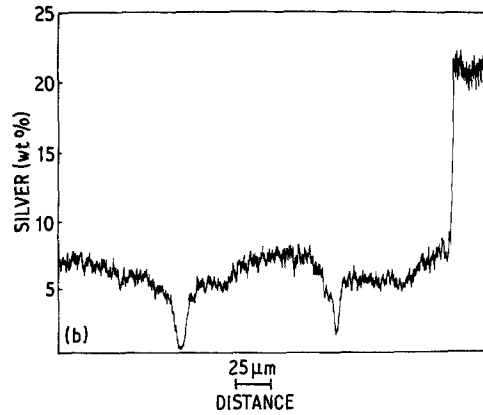
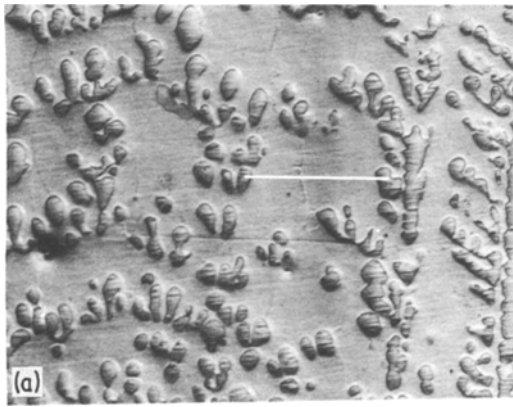


Figure 16 (a) Cd–8% Ag. Position of transverse trace at 330° C, just prior to complete solidification. $\times 90$. (b) Transverse trace showing a remnant of coring in the η phase and two “tails” of quenched liquid. An ϵ peak appears on the right.

line to lower silver contents. This involves a change in relative volume of the ϵ and η phases to approach equilibrium at each temperature.

6. Solid-state diffusion

A notable feature of the above observations is the rapid approach towards equilibrium in the solid state, even though the prevailing temperatures are quite low. An estimate of the diffusion coefficient for diffusion of silver in the η phase can be obtained from the time taken for the removal of the coring evident in Fig. 15. At 330° C the two minima in Fig. 15 represent η phase containing 1% silver adjacent to η phase containing 5% silver. At 320° C the η at the minima had been enriched to about 4% silver by diffusion from the adjacent η . Applying the standard solution of Fick's second law,

$$\frac{C_x - C_0}{C_s - C_0} = 1 - \operatorname{erf} \frac{x}{2D^{1/2}t}$$

where $C_s = 5.0$, $C_0 = 1.0$, $C_x = 4.0$, $x = 0.0015$ cm (half the width of the depleted region).

At a growth rate of $5 \mu\text{m sec}^{-1}$ the time taken to enrich the depleted region is less than 200 sec, for example 100 sec. Therefore,

$$\begin{aligned} D &= 9 \times 10^{-8} \text{ cm}^2 \text{ sec}^{-1} \\ &\simeq 1 \times 10^{-7} \text{ cm}^2 \text{ sec}^{-1} \end{aligned}$$

at 594° C.

This value is very close to $1.75 \times 10^{-7} \text{ cm}^2 \text{ sec}^{-1}$ for the diffusion of mercury in cadmium at 594° C, so that it is reasonable to use D_0 and Q as quoted for mercury in cadmium [5]:

$$D_0 = 2.57 \text{ cm}^2 \text{ sec}^{-1}$$

$$Q = 19.6 \text{ kcal mol}^{-1}$$

7. Conclusions

1. The steady-state solid–liquid interface profile in a directionally grown peritectic alloy is strongly dependent on the degree of participation of the peritectic transformation in the formation of the peritectic product. The properitectic primary phase will always grow as plates or dendrites lying more or less parallel to the heat flow direction, with their growth tips well in advance of a second interface formed by the peritectic product. In Cd–Cd₃Ag the peritectic product is formed almost entirely by the peritectic transformation and the second interface between two primary dendrites is formed by progressive thickening of peritectic envelopes until they meet. In Al–Al₃Ti the peritectic product is formed almost entirely by direct precipitation from the melt and the second interface tends to be planar, flanked by thin peritectic envelopes. Amongst other peritectic systems intermediate cases can be expected for which the second interface would approximate the concave profile predicted by Uhlmann and Chadwick [2].

2. In the Cd–Cd₃Ag system solid-state diffusion is sufficient to produce a close approach to equilibrium between the solid phases at room temperature, at the growth rates used. The diffusion coefficient for silver in the η phase is estimated from the rate of elimination of coring segregation.

Appendix

Unidirectional solidification was carried out in the vertical travelling furnace described in [6], using a crusilite element to give adequate temperature range. The growth rate could be varied between 5 and $200\ \mu\text{m sec}^{-1}$ with imposed temperature gradients up to $200^\circ\text{C cm}^{-1}$. Temperatures and temperature gradients were calibrated in dummy runs with a specimen containing a thermocouple, duplicating all conditions used in the subsequent experiments.

Direct cooling curves taken on the same alloys [7] provided an additional check. At the growth rates considered in this paper the cooling curve arrest at T_P occurred at the temperature predicted by the phase diagram, with no initial undercooling. During steady-state unidirectional solidification nucleation is not necessary, so the first appearance of peritectic product at the quenched interface should mark the T_P isotherm with some precision. Isotherms at points distant from T_P could then be determined using the temperature gradient calibration. Critical points so determined conformed closely with arrest temperatures on the direct cooling curves.

Electron probe microanalysis was carried out on a JEOL JXA-5A and a JEOL-JXA50A at different times. The spot size for point analysis was

approximately $1\ \mu\text{m}$ (except where otherwise specified in the text). For Al-Ti a correction curve for interference was prepared using a computer program [8]. The measured compositions, after correction, were estimated to be accurate to within $\pm 10\%$ at most, for example $0.5 \pm 0.05\%$ titanium. For Cd-Ag the same programme indicated that correction was unnecessary (Ag and Cd are adjacent in the periodic table). A similar accuracy was estimated.

References

1. W. J. BOETTINGER, *Met. Trans.* 5 (1974) 2023.
2. D. R. UHLMANN and G. A. CHADWICK, *Acta Metall.* 9 (1961) 835.
3. D. H. St. JOHN and L. M. HOGAN, *ibid.* 25 (1977) 77.
4. *Idem*, *J. Cryst. Growth* 46 (1979) 387.
5. C. J. SMITHELLS, "Metals Reference Book" Vol. 2 (Butterworth, London, 1967).
6. D. C. JENKINSON and L. M. HOGAN, *J. Cryst. Growth* 28 (1979) 171.
7. D. H. St. JOHN and L. M. HOGAN, *J. Mater. Sci.* 17 (1982) 2413.
8. J. W. COLBY, "Magic IV, A computer program for quantitative electron microprobe analysis" (Bell Telephone Laboratories Inc., Allentown, PA, USA, 1969).

*Received 8 April
and accepted 21 July 1983*